Built-in field reduction in InGaN/GaN quantum dot molecules

S. Schulz' and E. P. O'Reilly

Citation: Appl. Phys. Lett. **99**, 223106 (2011); doi: 10.1063/1.3665069
View online: http://dx.doi.org/10.1063/1.3665069
View Table of Contents: http://aip.scitation.org/toc/apl/99/22
Published by the American Institute of Physics

Built-in field reduction in InGaN/GaN quantum dot molecules

S. Schulz[1,a] and E. P. O'Reilly[1,2]
[1]*Tyndall National Institute, Lee Maltings, Cork, Ireland*
[2]*Department of Physics, University College Cork, Cork, Ireland*

(Received 23 September 2011; accepted 10 November 2011; published online 2 December 2011)

We use a tight-binding model to study the electronic structure of InGaN/GaN quantum dot molecules grown along the *c*-axis. This analysis is carried out as a function of the barrier thickness between the two non-identical dots. Our results show that the built-in field is effectively reduced in systems of coupled nitride quantum dots, leading to an increased spatial overlap of electron and hole wave functions compared to an isolated dot. This finding is in agreement with experimental data reported in the literature and is directly related to the behavior of the built-in potential outside an isolated dot. © *2011 American Institute of Physics*. [doi:10.1063/1.3665069]

The semiconductor materials InN, GaN, and AlN and their alloys have attracted considerable attention due to their promising applications in optoelectronic devices such as light-emitting diodes (LEDs) and laser structures.[1] Depending on the alloy composition, these systems are in principle able to cover a wide wavelength range from ultra-violet to infrared.[1] For energy-efficient solid state lighting, which combines output from blue, green, and red LEDs, InGaN alloys are promising candidates, since the assistance of phosphor is theoretically not required for a white light source.[1] While nitride-based heterostructures have already been utilized in blue LEDs (Ref. 2) and lasers,[3] the emission efficiency of *c*-plane InGaN/GaN quantum wells (QWs) drops significantly when going to longer wavelengths through the use of higher In composition or thicker QWs.[1] One of the main reasons for this behavior is the strong electrostatic built-in field in nitride-based heterostructures grown along the *c*-axis.[4]

One strategy to reduce the built-in field in nitride-based optoelectronic devices is to replace QWs by quantum dots (QDs), since the built-in potential in a QD compared to a QW of the same height and composition is significantly reduced.[5,6] The In composition can, therefore, be increased in a QD compared to a QW, enabling efficient recombination to longer wavelengths. Different authors[7] have recently demonstrated that InGaN-QD-based LEDs and lasers, operating in the amber and green spectral region, show superior performance compared to their QW-based counterparts. In the active region of the laser structures, stacks of InGaN QDs have been used.

Experimental data indicate that, compared to a single nitride QD, a vertical stacking of nitride dots leads to enhanced photoluminescence (PL) efficiency and efficient emission at room temperature.[8] Small barrier thicknesses ($D \approx 2$ nm) have been chosen to achieve a stronger coupling between the QDs along the *c*-axis.[8] In the experimental study in Ref. 9, the influence of the distance D between the dots in a stack of InGaN QDs was analyzed, showing that, with increasing D, the PL red-shifts and the PL lifetime increases. This indicates an increase in the magnitude of the built-in field with increasing D. Thus, understanding the mechanisms of inter-dot coupling is important not only for fundamental properties of coupled nitride QDs but also for designing nitride-based devices.

Here, we present a detailed analysis of the electronic structure of an InGaN/GaN QD molecule (QDM) based on a tight-binding (TB) model, and taking strain and built-in fields into account. The influence of the barrier thickness D between the two QDs is studied in detail. In the following, we consider QDs identical in size and shape but different in their composition. The difference in In composition mimics, therefore, already the effects (changes in confinement energy, strain, and built-in fields), which can also arise from a change in the QD geometry. Since the average diameter of InGaN QDs scatters around 15–25 nm while the average height is approximately 2–6 nm,[9,10] we assume a diameter $d \approx 19.2$ nm and a height $h \approx 3.1$ nm for both QDs. We assume here lens-shaped QD geometries.[10] There is no detailed measurement on the variation of the In content in stacked InGaN QDs. However, the analysis of coupled InGaAs QDs shows that, due to strain relaxation in the structure, the In composition of the upper QD is higher than in the lower one.[11] Since InGaN QD structures with 20%–25% In have been reported in the literature,[12] we assume an In content of 20% in the lower dot and 25% in the upper dot. Based on the experimental data in Ref. 13 and the discussions in Ref. 9, we assume a vertical stacking of the two QDs.

The electronic structure of this InGaN/GaN QDM is calculated using a sp^3 TB model.[14] The TB parameters for $In_xGa_{1-x}N$ are obtained from a modified virtual crystal approximation,[15] which allows us to take the band gap bowing into account. Such an approach has been often used to calculate the electronic structure of alloyed semiconductor materials.[15,16] The strain dependence of the TB matrix elements is included via the Pikus-Bir Hamiltonian[17] as a site-diagonal correction. In doing so, the relevant deformation potentials are included directly without any fitting procedure. The deformation potentials for InN and GaN are taken from Ref. 18, and a linear interpolation is used to obtain the parameters for $In_xGa_{1-x}N$. The built-in potential ϕ_p arising from spontaneous and piezoelectric polarization is also included as a site-diagonal contribution in the TB

[a]Author to whom correspondence should be addressed. Electronic mail: stefan.schulz@tyndall.ie.

Hamiltonian. Strain and polarization fields are calculated using a surface integral method,[19] with a linear interpolation for all parameters except for the spontaneous polarization, where we apply a quadratic interpolation.[20] When modeling the electronic structure of coupled c-plane nitride QDs, the sign of the shear piezoelectric coefficient e_{15} becomes important, since it affects the behavior of ϕ_p outside a single QD.[21] In the literature, positive as well as negative values are reported.[22] Our detailed analyses of wurtzite piezoelectric coefficients strongly support $e_{15} < 0$,[22] in agreement with recent experimental data.[23] We have, therefore, chosen $e_{15} < 0$.[21]

Here, we study the electronic structure of the InGaN QDM as a function of the barrier thickness D. In accordance with recent experimental data[9] on stacked InGaN QDs, we use the values of $D \approx 1$, 2, 4.1, 6.2, and 8.3 nm. In a first step, we look at the single-particle electron (ψ_1^e) and hole (ψ_1^h) ground state wave functions. Figure 1 shows the charge densities of ψ_1^e and ψ_1^h as a function of D. The light (blue) and dark (red) isosurfaces correspond to 10% and 50% of the maximum values, respectively. When looking at the results in detail, we find a ground state switching for the holes. For $D \approx 1$ nm, ψ_1^h is localized in the lower QD ($In_{0.2}Ga_{0.8}N$ QD) while ψ_1^e is localized in the upper dot ($In_{0.25}Ga_{0.75}N$ QD). For larger values of D, both ψ_1^h and ψ_1^e are localized on the upper dot. The reason for this switching originates from the behavior of the built-in potential ϕ_p above and below an isolated QD. Outside the QD, ϕ_p quickly returns to zero along the c-axis and changes sign a few nanometer away from the dot along the c-axis,[21] affecting, therefore, ϕ_p in a QDM. Line-scans through the center of the QDM along the c-axis for different D are shown in Fig. 2. The behavior of ϕ_p can be understood when superimposing built-in potentials of the two isolated QDs with their base centered at $z = 0$ and $z = h + D$, where h is the height of the lower QD.

The results for the isolated QDs are given by the dashed-dotted line and the dashed line, respectively. In the case of $D \approx 1$ nm (a), the magnitude of ϕ_p in the upper (lower) QD is reduced at the bottom (top), and almost unchanged at the top (bottom) compared to an isolated QD. Therefore, the electron wave functions could be expected to be localized at the top of the upper QD, while the hole states are expected to be localized at the bottom of the lower QD.

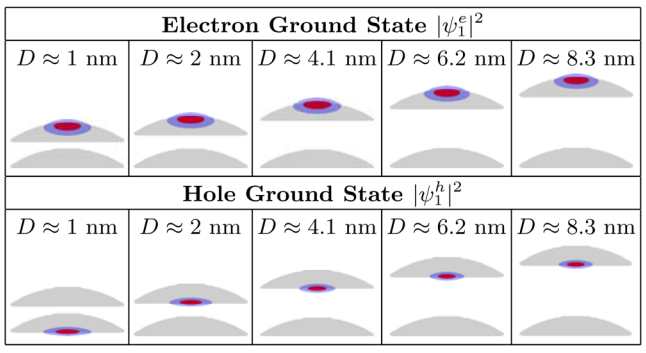

FIG. 1. (Color online) Probability densities of the electron and hole ground state wave functions ψ_1^e and ψ_1^h, respectively, for different barrier thicknesses D. The lens-shaped QD geometry is indicated by the shaded area. The light (blue) and dark (red) probability density isosurfaces correspond to 10% and 50%, respectively, of the maximum value. Upper QD: $In_{0.25}Ga_{0.75}N$; Lower QD: $In_{0.2}Ga_{0.8}N$.

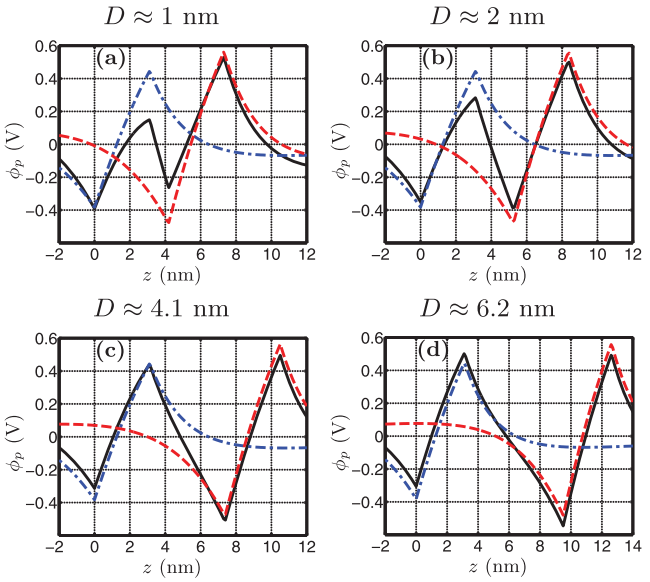

FIG. 2. (Color online) Built-in potential ϕ_p (solid black line) in a c-plane QDM of two non-identical QDs (lower QD: $In_{0.2}Ga_{0.8}N$; upper QD: $In_{0.25}Ga_{0.75}N$) for a line-scan through the center of the QDs along the c-axis and for different barrier thicknesses D between the QDs. The (blue) dashed-dotted line and the (red) dashed line indicate the results for isolated QDs.

This is exactly the result we obtain from our TB analysis [cf., Fig. 1]. For $D \geq 2$ nm, the change in sign in ϕ_p outside a single QD becomes important. For $D \geq 4.1$ nm, ϕ_p is slightly reduced in magnitude at the top (bottom) of the upper (lower) QD, while increased in magnitude at the bottom (top) of the upper (lower) QD [cf., Figs. 2(c) and 2(d)]. In the case of $D \approx 2$ nm, ϕ_p is decreased in magnitude at all four interfaces [cf., Fig. 2(b)]. From Figs. 2(b)–2(d), one could expect that ψ_1^e is localized at the top of the upper QD, while ψ_1^h is expected to be localized at the bottom of the upper QD. Again, this is in accordance with our TB results [cf., Fig. 1]. Note that the situation is different for two identical QDs. Here, ϕ_p breaks the symmetry between the dots. For the D values studied, ψ_1^e and ψ_1^h are always localized on different QDs (not shown), leading to a negligible spatial overlap, contrary to the experiment.[8,9]

The behavior of ϕ_p affects also the ground state transition energies $E_g^{\mathrm{QDM}} = E_1^e - E_1^h$, where E_1^e and E_1^h are ground state energies for electrons and holes, respectively. Figure 3 displays E_g^{QDM} as a function of D (dashed line). The result is compared to the transition energy E_g^{QD} of a single $In_{0.25}Ga_{0.75}N$ QD (dashed-dotted line). Figure 3 also displays the normalized squared dipole matrix element $|\tilde{d}_{11}|^2$ (solid line), defined by $|\tilde{d}_{11}|^2 = |d_{11}^{\mathrm{QDM}}|^2/|d_{11}^{\mathrm{QD}}|^2$, with $d_{11}^{\alpha} = \mathbf{e} \cdot \langle \psi_1^e | e_0 \mathbf{r} | \psi_1^h \rangle$, where $\mathbf{e} = 1/\sqrt{2}(1,1,0)$ is the light polarization vector and $e_0\mathbf{r}$ the dipole operator (e_0: electron charge). The dipole matrix elements of a single $In_{0.25}Ga_{0.75}N$ QD and the QDM are denoted by d_{11}^{QD} and d_{11}^{QDM}, respectively.

When looking at Fig. 3, we find that the energies E_g^{QDM} are blue shifted with respect to E_g^{QD}. This behavior can be attributed to the reduction of the biaxial compressive strain in the upper dot compared to an isolated QD. Additionally, an effective reduction of ϕ_p in the QDM compared to a single dot leads to a blue-shift in E_g^{QDM}. This effective reduction of ϕ_p also increases the spatial overlap of electron and hole

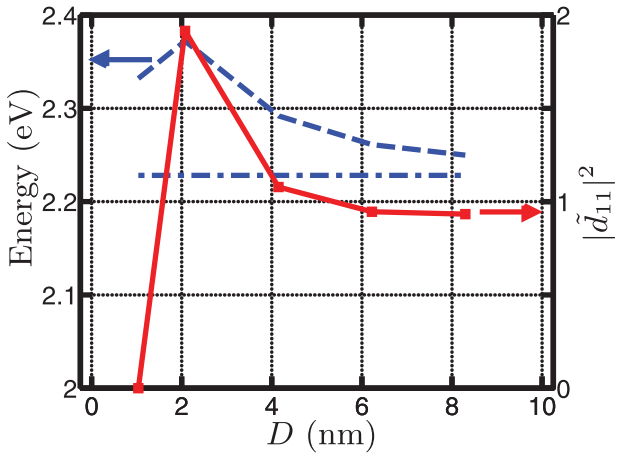

FIG. 3. (Color online) Single-particle energy gap for the InGaN QDM (dashed line) and an isolated $In_{0.25}Ga_{0.75}N$ QD (dashed-dotted line) as a function of the barrier thickness D. Solid line: Normalized dipole matrix element squared $|\tilde{d}_{11}|^2$.

wave functions so that $|\tilde{d}_{11}|^2 > 1$. Neglecting the results for $D \approx 1$ nm, where ψ_1^e and ψ_1^h are localized on different QDs [cf., Fig. 1], we find that, for $D \approx 2$ nm and $D \approx 4.1$ nm, $|\tilde{d}_{11}|^2 > 1$, indicating an effective reduction of ϕ_p in the upper dot. For example, for $D \approx 2$ nm, $|d_{11}^{\mathrm{QDM}}|^2$ is increased by a factor of order two compared to $|d_{11}^{\mathrm{QD}}|^2$, reflecting the change in the slope of ϕ_p in the upper dot of the QDM compared to an isolated QD [cf., Fig. 2(b)]. Please note that ϕ_p in an isolated QD is already significantly reduced compared to a QW structure of the same composition and height.[6] Therefore, the increase of $|\tilde{d}_{11}|^2$ for small D further emphasizes the benefit of using QDs instead of QWs in optoelectronic devices. It should be noted that $|\tilde{d}_{11}|^2 > 1$ for the ground state transition is a consequence of $e_{15} < 0$. With $e_{15} > 0$, as discussed in Ref. 21, ϕ_p in a QDM would be similar to the $D \approx 1$ nm case [Fig. 2(a)]. Since $|\tilde{d}_{11}|^2 > 1$ is in qualitative agreement with the experiment,[8,9] this further supports our earlier conclusion that $e_{15} < 0$.[22] For larger values of D ($D > 5$ nm), $|\tilde{d}_{11}|^2$ drops below unity. Looking at $D \approx 6.2$ nm, the slope of ϕ_p inside the upper dot is almost identical to the slope inside a single QD [cf., Fig. 2(d)]. However, the magnitude of ϕ_p at bottom (top) of the upper dot is slightly increased (decreased) compared to an isolated QD. This increased (decreased) ϕ_p leads to an increased (decreased) lateral confinement for ψ_1^h (ψ_1^e), resulting in $|\tilde{d}_{11}|^2 < 1$ for $D > 5$ nm.

In summary, we have presented a detailed analysis of the electronic structure of c-plane InGaN QDMs made up of two non-identical QDs, including, in particular, an analysis of the influence of the barrier thickness between the two QDs. Our study revealed that the built-in field in a QDM can be effectively reduced compared to a single QD, leading to an increase in the spatial overlap of electron and hole wave functions. These results are in qualitative agreement with experimental data[8,9] for stacked nitride QDs, where PL measurements show reduced recombination lifetimes indicative of an increased spatial overlap of electron and hole wave functions. Furthermore, due to the behavior of the built-in field in a system of stacked QDs, the distance between the two QDs can be used to engineer the optical recombination rate. Therefore, our analysis indicates the potential of stacked nitride QDs for high efficiency light emitters with high In content.

The work was supported by Science Foundation Ireland.

[1] C. J. Humphreys, MRS Bull. **33**, 459 (2008).
[2] S. Nakamura, T. Mukai, and M. Senoh, Appl. Phys. Lett. **64**, 1687 (1994).
[3] S. Nakamura, IEEE J. Sel. Top. Quantum. Electron. **3**, 712 (1997).
[4] J. Simon, N. T. Pelekanos, C. Adelmann, E. Martinez-Guerrero, R. Andre, B. Daudin, L. S. Dang, and H. Mariette, Phys. Rev. B **68**, 035312 (2003).
[5] Y.-R. Wu, Y.-Y. Lin, H.-H. Huang, and J. Singh, J. Appl. Phys. **105**, 013117 (2009).
[6] S. Schulz and E. P. O'Reilly, Phys. Rev. B **82**, 033411 (2010).
[7] M. Zhang, P. Bhattacharya, and W. Guo, Appl. Phys. Lett. **97**, 011103 (2010); C. B. Soh, W. Liu, S. J. Chua, S. S. Ang, R. J. N. Tan, and S. Y. Chow, J. Appl. Phys. **108**, 093501 (2010); M. Zhang, A. Banerjee, C.-S. Lee, J. M. Hinckley, and P. Bhattacharya, Appl. Phys. Lett. **98**, 221104 (2011).
[8] A. Neogi, H. Morkoc, T. Kuroda, A. Tackeuchi, T. Kawazoe, and M. Ohtsu, Nano Lett. **5**, 213 (2004).
[9] S. C. Davies, D. J. Mowbray, F. Ranalli, and T. Wang, Appl. Phys. Lett. **96**, 251904 (2010).
[10] M. Senes, K. L. Smith, T. M. Smeeton, S. E. Hooper, and J. Heffernan, Phys. Rev. B **75**, 045314 (2007); O. Moriwaki, T. Someya, K. Tachibana, S. Ishida, and Y. Arakawa, Appl. Phys. Lett. **76**, 2361 (2000).
[11] Q. Zhang, J. Zhu, X. Ren, H. Li, and T. Wang, Appl. Phys. Lett. **78**, 3830 (2001).
[12] J. W. Robinson, J. H. Rice, K. H. Lee, J. H. Na, R. A. Taylor, D. G. Hasko, R. A. Oliver, M. J. Kappers, C. J. Humphreys, and G. A. D. Briggs, Appl. Phys. Lett. **86**, 213103 (2005).
[13] A. Neogi, B. P. Gorman, H. Morkoc, T. Kawazoe, and M. Ohtsu, Appl. Phys. Lett. **86**, 043103 (2005).
[14] S. Schulz, S. Schumacher, and G. Czycholl, Eur. Phys. J. B **64**, 51 (2008).
[15] S. J. Lee, H. S. Chung, K. Nahm, and C. K. Kim, Phys. Rev. B **42**, 1452 (1990).
[16] B. Bouhafs, A. Aourag, M. Ferhat, A. Zaoui, and M. Certier, J. Appl. Phys. **82**, 4923 (1997); A. B. Fredj, M. Debbichi, and M. Said, Microelectron. J. **38**, 860 (2007).
[17] M. Winkelnkemper, A. Schliwa, and D. Bimberg, Phys. Rev. B **74**, 155322 (2006).
[18] Q. Yan, P. Rinke, M. Scheffler, and C. G. Van de Walle, Appl. Phys. Lett. **95**, 121111 (2009).
[19] D. P. Williams, A. D. Andreev, E. P. O'Reilly, and D. A. Faux, Phys. Rev. B **72**, 235318 (2005).
[20] I. Vurgaftman and J. R. Meyer, J. Appl. Phys. **94**, 3675 (2003).
[21] S. Schulz and E. P. O'Reilly, Phys. Status Solidi A **208**, 1551 (2011).
[22] S. Schulz, A. Berube, and E. P. O'Reilly, Phys. Rev. B **79**, 081401(R) (2009); S. Schulz, M. A. Caro, E. P. O'Reilly, and O. Marquardt, Phys. Rev. B **84**, 125312 (2011).
[23] H. Shen, M. Wraback, H. Zhong, A. Tyagi, S. P. DenBaars, S. Nakamura, and J. S. Speck, Appl. Phys. Lett. **95**, 033503 (2009).